13th World Conference on Earthquake Engineering
Vancouver, B.C., Canada
August 1-6, 2004
Paper No. 2368

ASSESSMENT OF SOIL NONLINEARITY USING EMPIRICAL GREEN'S FUNCTION METHOD

Atsushi NOZU[1] and Hitoshi MORIKAWA[2]

SUMMARY

The effects of soil nonlinearity in the Seattle Basin during the 2001 Nisqually, Washington, earthquake were assessed by using the empirical Green's function method. At some of the stiff-soil sites, it was estimated that the amplitudes of the later phases were reduced due to a small increase in damping factor along the seismic ray in the sediments. The effects of soil nonlinearity on the later phases were much more prominent at soft-soil sites. Efforts are needed to establish a reasonable way to evaluate such effects in the prediction of strong ground motions at sites in a sedimentary basin.

INTRODUCTION

Evaluation of the effects of soil nonlinearity is an important issue for the prediction of strong ground motions [1,2]. The authors [3] have been developing a simple method to incorporate soil nonlinearity within the framework of the conventional empirical Green's function method [4,5]. The method requires two additional parameters; one represents the averaged reduction in shear wave velocity and the other represents the averaged increase in damping factor in the sediments through which the seismic ray passes before reaching the site. These parameters, which are referred to as "nonlinear parameters", are used to modify the empirical Green's functions in time domain. By using the method, one can assess the effects of soil nonlinearity during the past events. The procedure is as follows; first, a source model is constructed that can explain ground motions at stations that are free from soil nonlinearity. Secondly, the same source model is applied to stations that are potentially affected by soil nonlinearity without consideration of soil nonlinearity. Finally, if a discrepancy is found in the second step between the synthetic and the recorded ground motions, a try-and-error approach is used to find appropriate "nonlinear parameters" to explain the records at the sites. Thus one can estimate the deviation of material properties of the sediments due to soil nonlinearity from linear status. In this article, the method is applied to the records obtained in the Seattle Basin [6] during the 2001 Nisqually, Washington, earthquake (M_W6.8) to assess the effects of soil nonlinearity on the mainshock ground motions.

METHOD

[1] Senior Research Engineer, Port and Airport Research Institute, Japan
[2] Associate Professor, Tokyo Institute of Technology, Japan

When the site under consideration is in a sedimentary basin, seismic rays connecting the source and the site can be trapped within the basin as illustrated in **Figure 1**. In the empirical Green's function method, it is assumed that the rays are shared between the large and the small events.

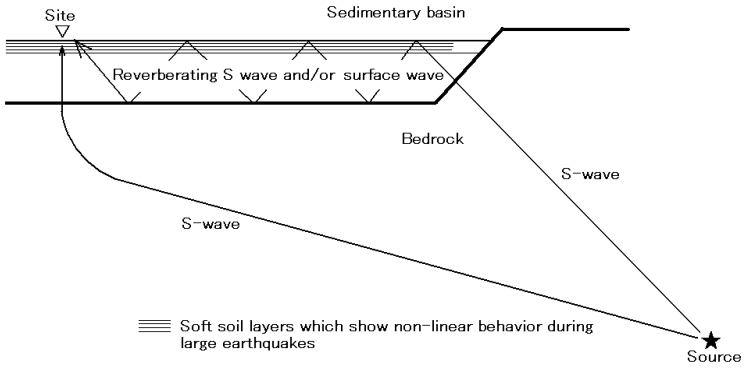

Figure 1. An example of a seismic ray trapped within the sedimentary basin.

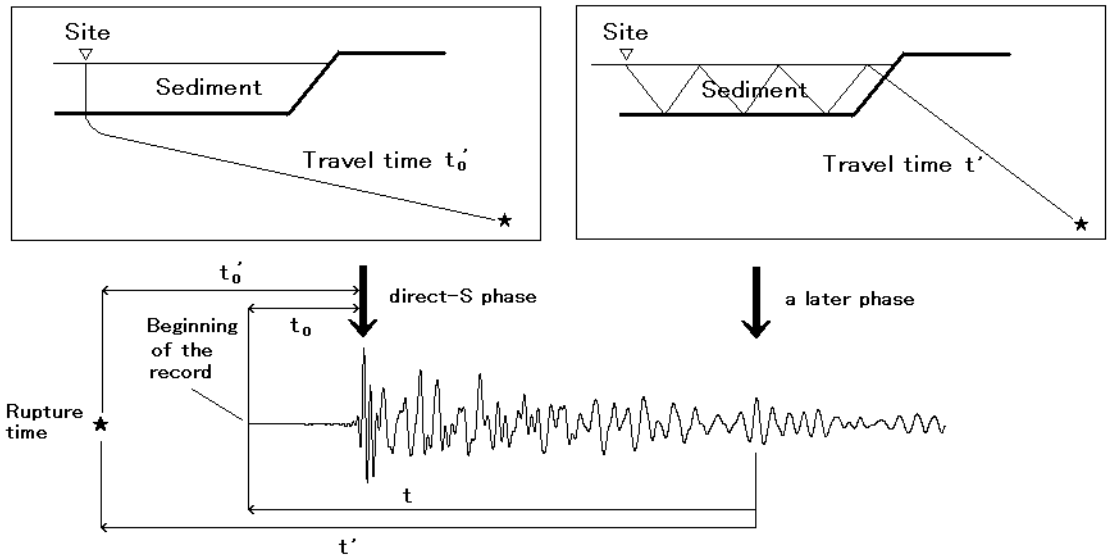

Figure 2. Plausible seismic rays corresponding to the direct-S phase and an arbitrary later phase on a Green's function.

The present method [3] is an extended version of the conventional empirical Green's function method to incorporate the effects of soil nonlinearity. One of the key assumption in the present method is that the delay of an arbitrary later phase found on the Green's function is caused by the trapping of the seismic ray within the sedimentary basin as schematically illustrated in **Figure 2**. In other words, it is assumed that the site effects, rather than the path effects, are predominant in the phase information of the Green's function. Thus the difference of arrival times of the direct-S phase and the later phase on the Green's

function $t-t_0$ is approximately equal to the time for which the seismic ray corresponding to the later phase is trapped within the sedimentary basin. It is important in this discussion that the time history in **Figure 2** should be a Green's function instead of a mainshock ground motion. Because the source time function for a Green's function is impulsive, different arrivals found on the Green's function can be regarded to have started the hypocenter at the same time and, therefore, difference in arrival times can be attributed to the difference of time spent along the ray.

In case of a strong excitation, the materials within the sedimentary basin can exhibit nonlinear behavior including the reduction in shear wave velocity and the increase in damping [2]. The nonlinear behavior is typically most prominent near the surface of the basin as illustrated in **Figure 1**. Due to the nonlinear behavior, the arrival time of a later phase will be delayed and the amplitude of the later phase will be reduced. To represent these effects, two parameters, ν_1 and ν_2, are introduced to represent the deviation of material properties of the sediments from linear status due to soil nonlinearity. The parameter ν_1 is defined as the averaged reduction in shear wave velocity along the ray in the sediments, that is, $\nu_1 = Vs/Vs_0$, where Vs is the shear wave velocity for a strong motion and Vs_0 is the shear wave velocity for a weak motion. The parameter ν_2 is defined as the averaged increase in damping factor along the ray in the sediments, that is, $\nu_2 = h-h_0$, where h is the damping factor for a strong motion and h_0 is the damping factor for a weak motion. Then, in case of a strong excitation, the seismic ray corresponding to the later phase will be trapped within the sedimentary basin $1/\nu_1$ times longer than the linear case. At the same time, the amplitude of the later phase will be reduced by a factor of $\exp[-\nu_2\ \omega(t-t_0)]$, because $t-t_0$ is approximately equal to the time for which the seismic ray corresponding to the later phase is trapped within the sedimentary basin as discussed above. As a result, the Green's function is modified as follows:

$$g_n(t)=g(t) \quad \text{for } t<t_0 \text{ and}$$
$$g_n(t_0+(t-t_0)/\nu_1)=g(t)\exp[-\nu_2\ \omega(t-t_0)] \quad \text{for } t>t_0, \qquad (1)$$

where $g(t)$ is the original Green's function and $g_n(t)$ is the Green's function after modification. The parameters ν_1 and ν_2 will be referred to as "the nonlinear parameters" in the present article. In practice, if the Green's function is narrow-band, the corresponding angular frequency can be used in equation (1). If the Green's function is broad-band, the function should be, at first, decomposed into components having different frequencies and then each component should be modified in the same manner as in the narrow-band case. Finally, the modified components should be summed up. The parameter ν_2 can be either constant or frequency-dependent. Although the authors adopted a constant ν_2 in the previous applications [3], it was found that a frequency-dependent ν_2 is more preferable in the present application to the Nisqually earthquake. In this study, the parameter ν_2 is assumed to be proportional to frequency, that is, $\nu_2 \propto f$.

The present analysis using the nonlinear parameters may be regarded as an extension of the conventional equivalent-linear analysis [7] that has been widely employed in the field of geotechnical engineering. In the equivalent-linear analysis, it is assumed that the material of the ground can be represented as a linear visco-elastic body. The parameters that characterize the visco-elastic body are assumed to be time-independent, although different parameters are assumed for weak and strong ground motions. These assumptions are also adopted in the present analysis. The difference between the present analysis and the conventional equivalent-linear analysis is that, while deviation of material properties from linear status for each soil layer or each soil element was the issue for the conventional analysis, deviation of material properties averaged along the seismic ray in the sediments is the issue for the present analysis. Of course, nonlinearity of the media is, in fact, time-dependent. The dependence is neglected for simplicity in the present analysis as is done in the conventional equivalent-linear analysis.

The method can be used to assess the effects of soil nonlinearity during the past events in time domain. The procedure is as follows; first, a source model is constructed that can explain the ground motions at stations that are presumably free from soil nonlinearity. Secondly, the same source model is applied to stations that are potentially affected by soil nonlinearity without consideration of soil nonlinearity. Finally, if a discrepancy is found in the second step between the synthetic and the recorded ground motions, a try-

and-error approach is used to find appropriate "nonlinear parameters" to explain the records at the sites. Thus one can estimate the deviation of material properties of the sediments from linear status due to soil nonlinearity.

RECORDINGS FROM THE NISQUALLY EARTHQUAKE

The M_W6.8 Nisqually, Washington, earthquake of February 28, 2001 (18:54:32 UTC, d=52km) and its M_L3.4 aftershock (March 1, 2001, 9:10:20 UTC, d=54km) were recorded on a variety of surficial geological units in Seattle [6]. The sites that recorded the earthquakes include those on artificial fill, Holocene alluvium, modified land, Pleistocene stiff soils and Tertiary sedimentary rock. Frankel et al. [6] analyzed the data and found indications of nonlinear soil behavior at soft-soil sites on artificial fill and Holocene alluvium. Their analysis was conducted mainly in frequency domain by using spectral ratio technique. In the present article, the authors' intention is to assess soil nonlinearity in time domain.

Figure 3 indicates twelve observation stations from the Seattle Urban Seismic Array of the U.S. Geological Survey (http://groundmotion.cr.usgs.gov) used for the present analysis. The sites HAR, SDN and SDS are located on artificial fill. The sites BHD, SEU, THO, CTR, HIG, CRO, LAP, HAL and EVA are located on Pleistocene stiff soils. Features of the stations are summarized in **Table 1**. Peak ground velocities listed in **Table 1** are those for radial components during the mainshock. Besides the surficial geology, another important issue for these sites is that the sites are located in the Seattle Basin. Because of this fact, basin surface waves were observed during the mainshock at these sites [6]. This fact plays an important role in the interpretation of the data at these sites. In **Figure 3**, the dotted line indicates the approximate location of the Seattle fault, which forms the southern edge of the Seattle Basin [6].

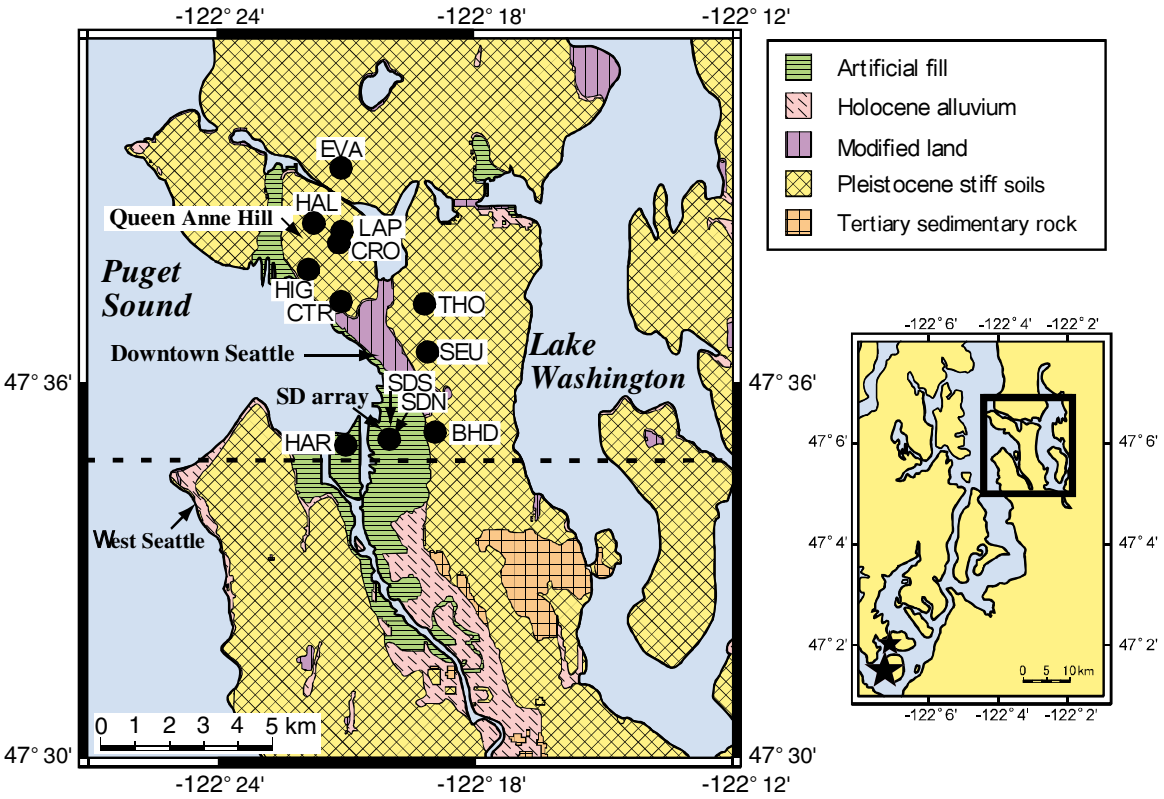

Figure 3 Stations used in this study, surficial geology [6] and epicenters (stars in the right panel).

Table 1 Stations used for the analysis.

Station Name	Latitude (degrees)	Longitude (degrees)	Elevation (meters)	Soil Type	PGV (cm/s)
BHD	47.5864	-122.3158	95	Pleistocene stiff soils	18.0
SEU	47.6078	-122.3178	88	Pleistocene stiff soils	6.1
THO	47.6205	-122.3190	100	Pleistocene stiff soils	6.1
CTR	47.6207	-122.3514	43	Pleistocene stiff soils	8.3
HIG	47.6292	-122.3641	98	Pleistocene stiff soils	7.5
CRO	47.6371	-122.3514	117	Pleistocene stiff soils	7.4
LAP	47.6393	-122.3505	113	Pleistocene stiff soils	10.3
HAL	47.6418	-122.3616	83	Pleistocene stiff soils	10.0
EVA	47.6557	-122.3509	59	Pleistocene stiff soils	6.9
HAR	47.5837	-122.3501	4	Artificial fill	27.5
SDN	47.5856	-122.3315	5	Artificial fill	30.9
SDS	47.5833	-122.3315	5	Artificial fill	37.9

Frankel [6] pointed out that response at stiff-soil sites was approximately linear during the mainshock based on spectral ratio analysis. It was decided, therefore, that the records at stiff-soil sites should be used for the waveform inversion in this study to construct a source model for use in the empirical Green's function method. The later phases were excluded, however, from the inversion because the later phases might be more susceptible to soil nonlinearity. The effects of soil nonlinearity on the later phases at these sites will be discussed in the ensuing sections. For stations on artificial fill, Frankel [6] found several indications of nonlinear response including a clear shift of the resonant frequency, cusped accelerograms after the S wave and amplification at 10-20 Hz in the S wave. More information can be found in [6] and also at the web site of the U.S. Geological Survey (see http://groundmotion.cr.usgs.gov).

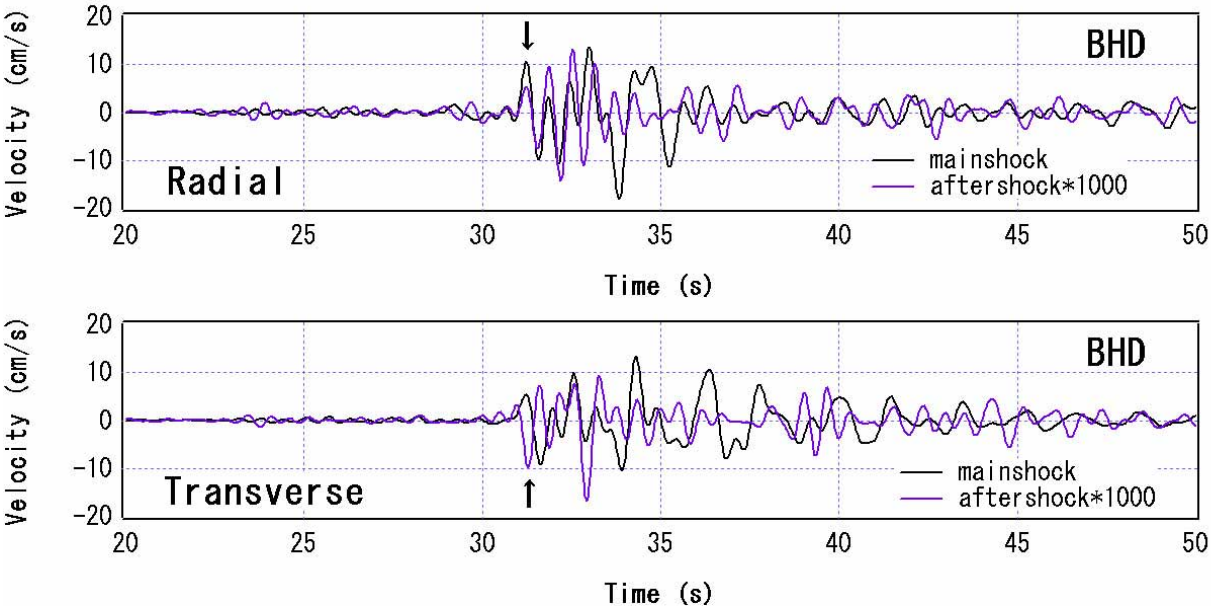

Figure 4 Radial and transverse velocities at BHD for the mainshock and the aftershock.

Components used for the analysis was decided as follows. In **Figure 4**, radial and transverse velocities at BHD are compared between the mainshock and the aftershock. The aftershock velocities are multiplied by 1000 and shifted to align its S wave with that for the mainshock. Unfortunately a discrepancy is found in the polarity of the initial S wave between the mainshock and the aftershock for the transverse component. This might be due to a difference between the mainshock and the aftershock focal mechanisms. Because it is not reasonable to model the transverse component by using the empirical Green's function method in this case, it was decided that only the radial components should be modeled in the ensuing analysis.

SOURCE MODEL OF THE NISQUALLY EARTHQUAKE

First, a waveform inversion was conducted to construct a variable-slip rupture model of the earthquake for use in the empirical Green's function method. The records of the M_L3.4 aftershock were used as the Green's functions. The epicenters of the mainshock (47.15N, 122.72W) and the aftershock (47.19N, 122.71W) are also shown in **Figure 3**. Because of the large distance to the hypocenters from the sites considered, a source model constructed for some of the sites should be valid for sites that are not used in the inversion. This point will be further discussed at the end of this section. Five of the sites on Pleistocene stiff soil, namely, BHD, SEU, THO, LAP and CTR are used for the inversion. Records at the soft/hard rock sites ALK, BRI and SEW [6] were excluded from the inversion because the amplitude during the aftershock at these sites was fairly small and therefore S/N ratio for these sites might not be excellent. The mainshock accelerograms were band pass filtered between 0.4 to 2.0 Hz and integrated in the frequency domain to obtain velocity waveforms. Original NS and EW components were rotated to obtain radial components. The aftershock accelerograms were processed in the same way to obtain velocity waveforms, which are used as the empirical Green's functions.

These sites are located on Pleistocene stiff soils (NEHRP classes D and C) and, according to Frankel [6], response at these sites was approximately linear during the mainshock. It was assumed, therefore, that the S waves observed at these sites during the mainshock were not affected by soil nonlinearity. The later phases were excluded, however, from the inversion because later phases might be more susceptible to soil nonlinearity as shown in **Figure 1**. Thus it was decided that portions of the mainshock records with duration of 5 seconds including the S waves should be used for the inversion (hatched portions in **Figure 5**).

The conventional least-squares linear waveform inversion [8] was adopted. Fault plane with a dimension of 30km times 30km was assumed, whose strike and dip angles were set to be 1° and 62°, respectively, referring to the CMT solution provided by the Earthquake Research Institute, the University of Tokyo (see http://kea.eri.u-tokyo.ac.jp/EIC/EIC_News). The fault was divided into 30 times 30 fault elements. The rupture front is assumed to start from the hypocenter at 18:54:32 UTC and to propagate radially at a constant velocity of 2.8km/s. Each fault element is allowed to slip four times in 1.2 seconds after passage of the rupture front at equal time intervals. The moment release of each slip relative to the moment of the aftershock was determined through the inversion. Conventional corrections for the geometrical spreading and time shifts [5] were applied to the empirical Green's functions to represent arrivals from each fault element. Absolute time information for both the mainshock and the aftershock recordings was used. In the inversion analysis, constraints were imposed to minimize the second order derivative of the slip on the fault with respect to time and space. Non-negative least-square solutions were obtained by using the algorithm of Lowson [9].

The synthetic mainshock velocities (0.4-2.0 Hz) as a result of the inversion were compared with the observed ones in **Figure 5**. Although the inversion determines the moment release on the fault relative to the aftershock moment, by assuming that the aftershock moment magnitude is approximated by its local magnitude, final slip distribution on the fault was roughly estimated as shown in **Figure 6**. The moment magnitude corresponding to the slip model in **Figure 6** is M_W 6.7, which is slightly smaller than the value

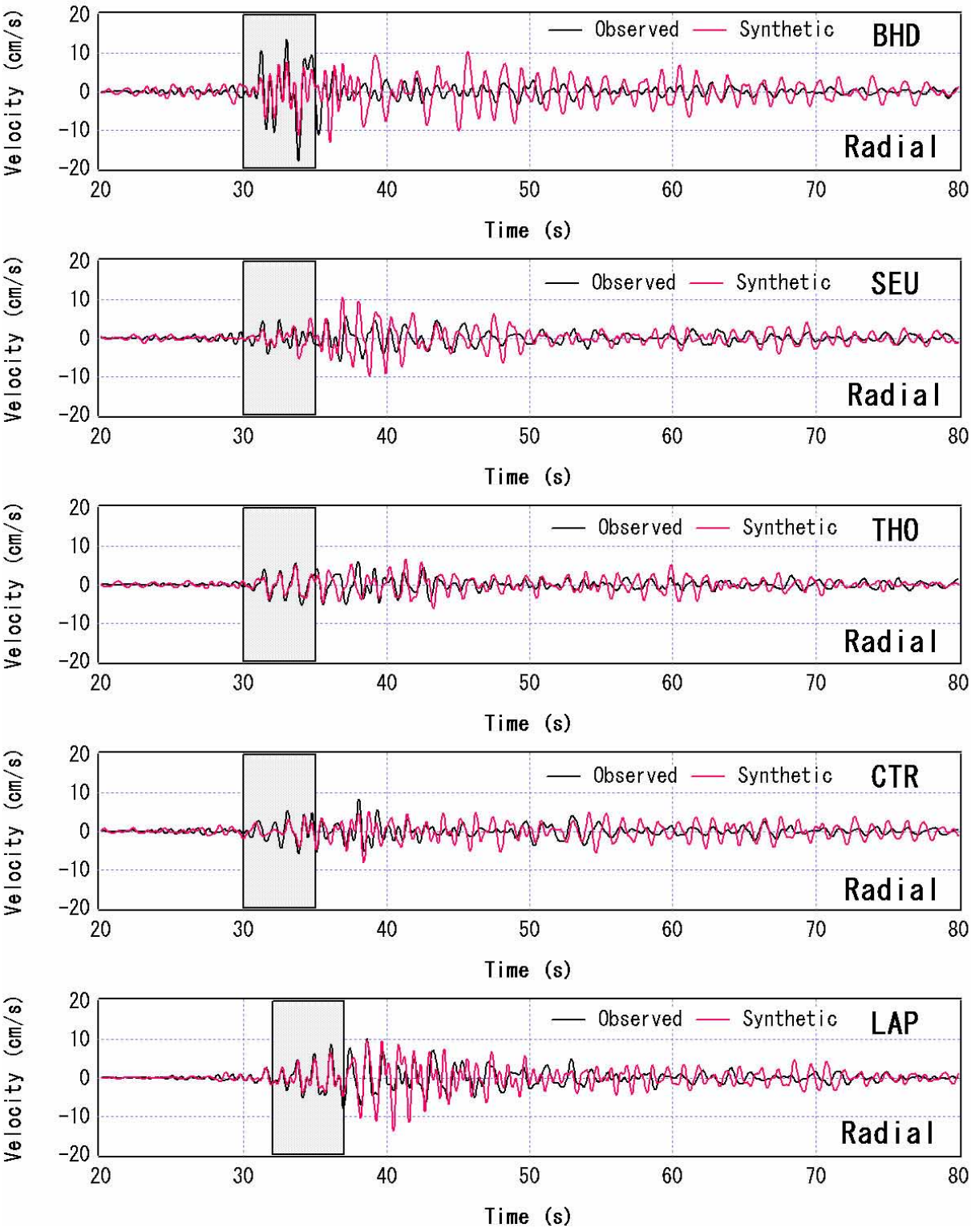

Figure 5 Observed and synthetic ground velocities at sites used for the inversion. Soil nonlinearity is neglected in the simulation.

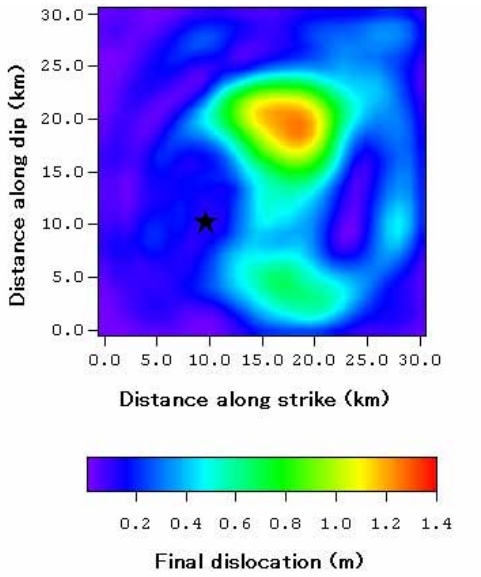

Figure 6 Approximate final slip distribution of the 2001 Nisqually, Washington, earthquake.

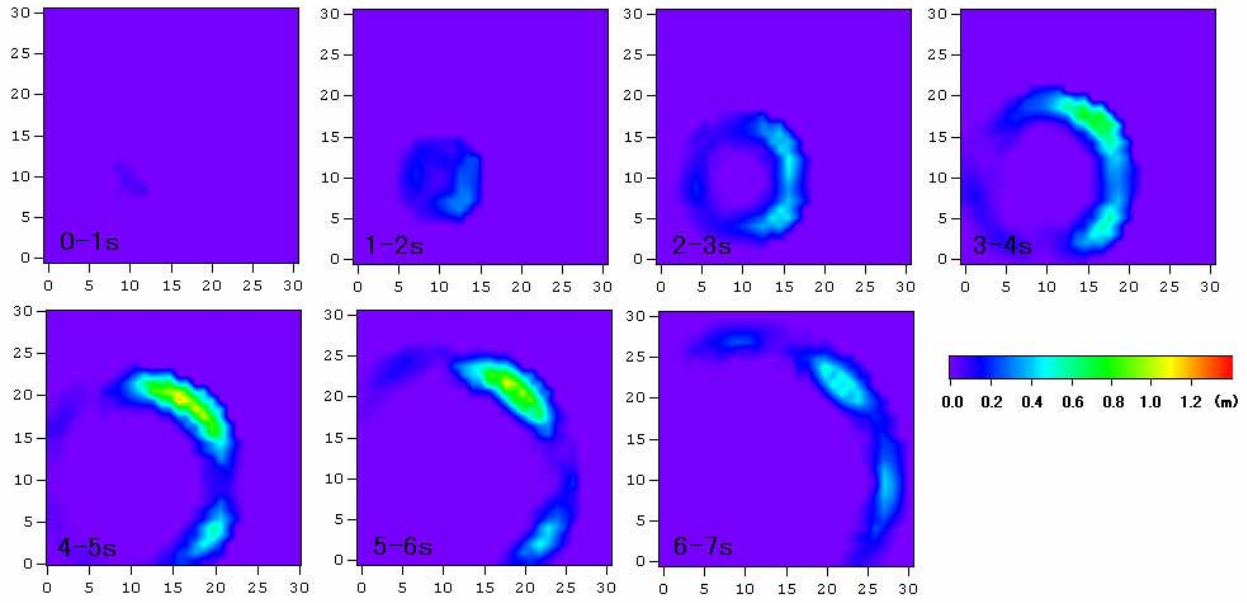

Figure 7 Approximate slip for each time window during the 2001 Nisqually, Washington, earthquake.

obtained by the USGS (M_W 6.8). The slip model is characterized by two asperities, with a major asperity located approximately 10km away from the hypocenter (the hypocenter is indicated by a star). **Figure 7** shows the approximate slip for each time window of 1 second during the earthquake.

As can be seen in **Figure 5**, agreement between the waves is satisfactory for portions that were used for the inversion (hatched portions). For the later phases, however, the amplitudes are overestimated. This could be symptomatic of the effects of nonlinear soil behavior along the ray trapped within the sedimentary basin (see **Figure 1**). This point will be further discussed in the next section. Because the S

wave portions are satisfactory reproduced with this model, the authors consider that the model thus obtained (**Figure 6**) is the most plausible model that can be deduced from the data used.

For the purpose of testing the reliability of the model, ground motion velocities were synthesized and compared with observed velocities at sites on Pleistocene stiff soils that were not included in the waveform inversion. **Figure 8** shows the results for sites HIG, CRO, HAL and EVA. Agreement is satisfactory for portions that include the initial S waves (hatched portions), indicating the validity of the model. The large distance to the hypocenters from the sites under consideration seems to be a contributing factor to the result. For the later phases, again, the amplitudes are overestimated. Cause of the discrepancy will be discussed in the next section.

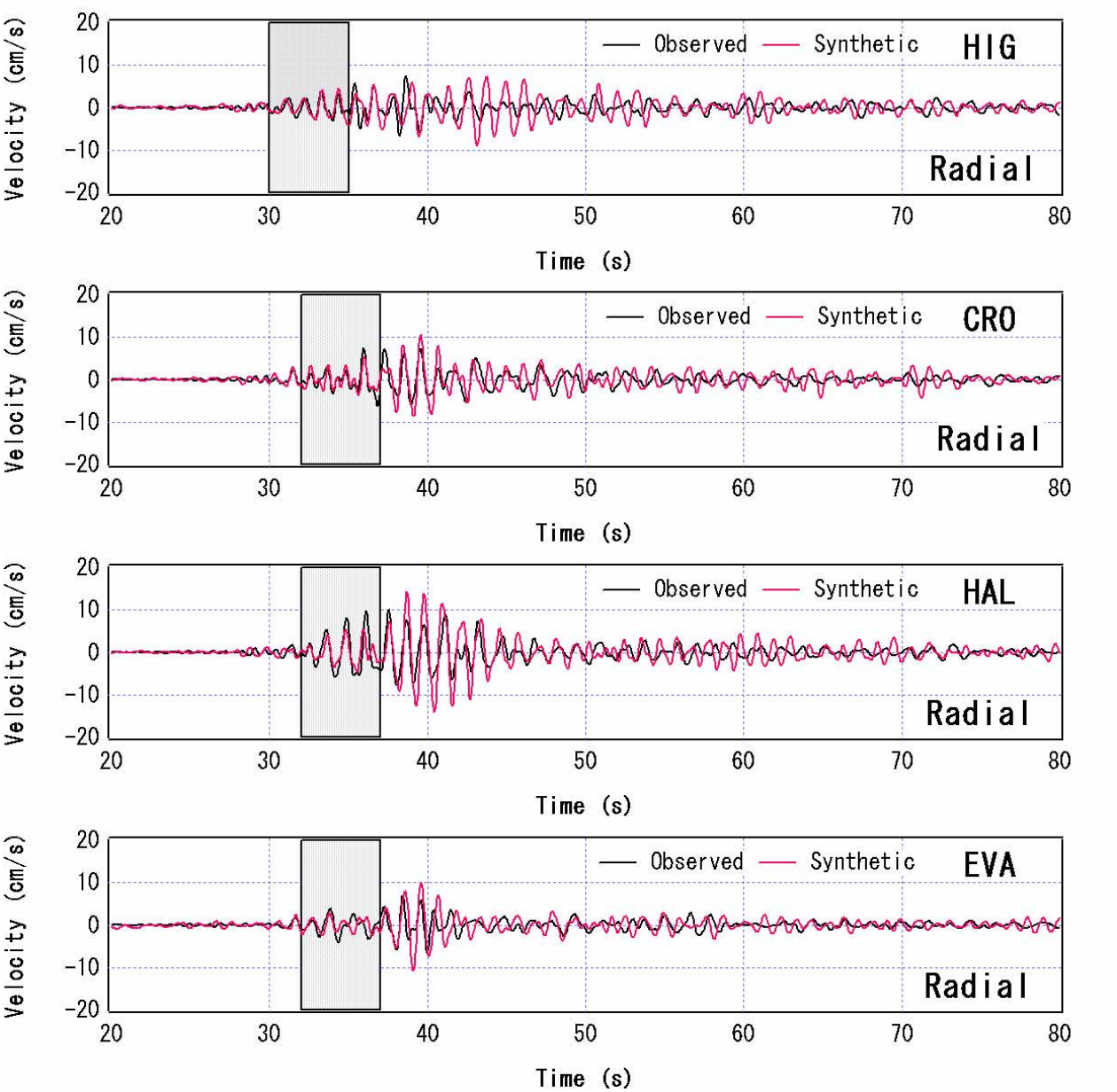

Figure 8 Observed and synthetic ground velocities at stiff-soil sites that are not used for the inversion. Soil nonlinearity is neglected in the simulation.

ASSESMENT OF SOIL NONLINEARITY

In this section, based on the source model obtained above, the effects of soil nonlinearity during the Nisqually mainshock are assessed by using the proposed method.

Sites on Pleistocene stiff soils

In the previous section, discrepancies are already found between the observed and the synthetic ground velocities for the later phases at some of the Pleistocene stiff-soil sites. Frankel [6] pointed out that the later phases found in these records correspond to basin surface waves in the Seattle Basin. Because the ray corresponds to the later phases tend to stay within the sediment for a long time (see **Figure 1**), the discrepancy is symptomatic of the nonlinear soil behavior along the ray trapped within the sedimentary basin. The authors, therefore, tried to simulate ground velocities at these sites by using the present method to incorporate soil nonlinearity. A try-and-error approach was adopted to find appropriate "nonlinear parameters" to explain the records at these sites. The results are summarized in **Table 2**. Synthetic velocities at five stiff-soil sites using the nonlinear parameters listed in **Table 2** are compared with the observed ones in **Figure 9**. Coincidence between the observed and synthetic ground velocities is satisfactory. If we compare the result with the previous result in which soil nonlinearity is neglected (**Figure 5** and **Figure 8**), it is clear that the results were improved by incorporating "nonlinear parameters". This makes us confident that the discrepancies found in the later phases in **Figure 5** and **Figure 8** should be due to nonlinear soil behavior along the ray trapped within the sedimentary basin. It should be noted that, except for BHD and SEU, the value is no more than 0.005, which by definition corresponds to an increase of 0.005 in the damping factor averaged along the seismic ray that passes through the sediments before arriving at these sites. Such a small change in the damping factor can affect the amplitude of the later phases easily because the ray corresponding to the later phases are trapped within the sedimentary basin for a long time. In another words, later phases are more susceptible to soil nonlinearity than S waves. It should be noted that the discrepancy in the waveforms found on the linear analysis (**Figure 5** and **Figure 8**) does not necessary imply that the response of the soil just beneath the sites was nonlinear. It just implies that some of the materials along the ray within the sediments showed nonlinear behavior. At BHD and SEU, a relatively small ν_1 and a relatively large ν_2 were identified, although these sites are also located on Pleistocene stiff soils. This may imply that, because these sites are closer to the artificial fill near downtown, some of the ray corresponding to the later phases at these stations passed through the artificial fill, where soil nonlinearity was prominent.

Table 2. Appropriate nonlinear parameters identified for each station (ν_2 is the value at 1 Hz).

Station Name	Soil type	PGV (cm/s)	ν_1	ν_2
BHD	Pleistocene stiff soils	18.0	0.68	0.050
SEU	Pleistocene stiff soils	6.1	0.89	0.010
THO	Pleistocene stiff soils	6.1	1.00	0.005
CTR	Pleistocene stiff soils	8.3	1.00	0.005
HIG	Pleistocene stiff soils	7.5	1.00	0.005
CRO	Pleistocene stiff soils	7.4	1.00	0.005
LAP	Pleistocene stiff soils	10.3	1.00	0.005
HAL	Pleistocene stiff soils	10.0	1.00	0.005
EVA	Pleistocene stiff soils	6.9	1.00	0.005
HAR	Artificial fill	27.5	0.66	0.020
SDN	Artificial fill	30.9	0.68	0.060
SDS	Artificial fill	37.9	0.65	0.060

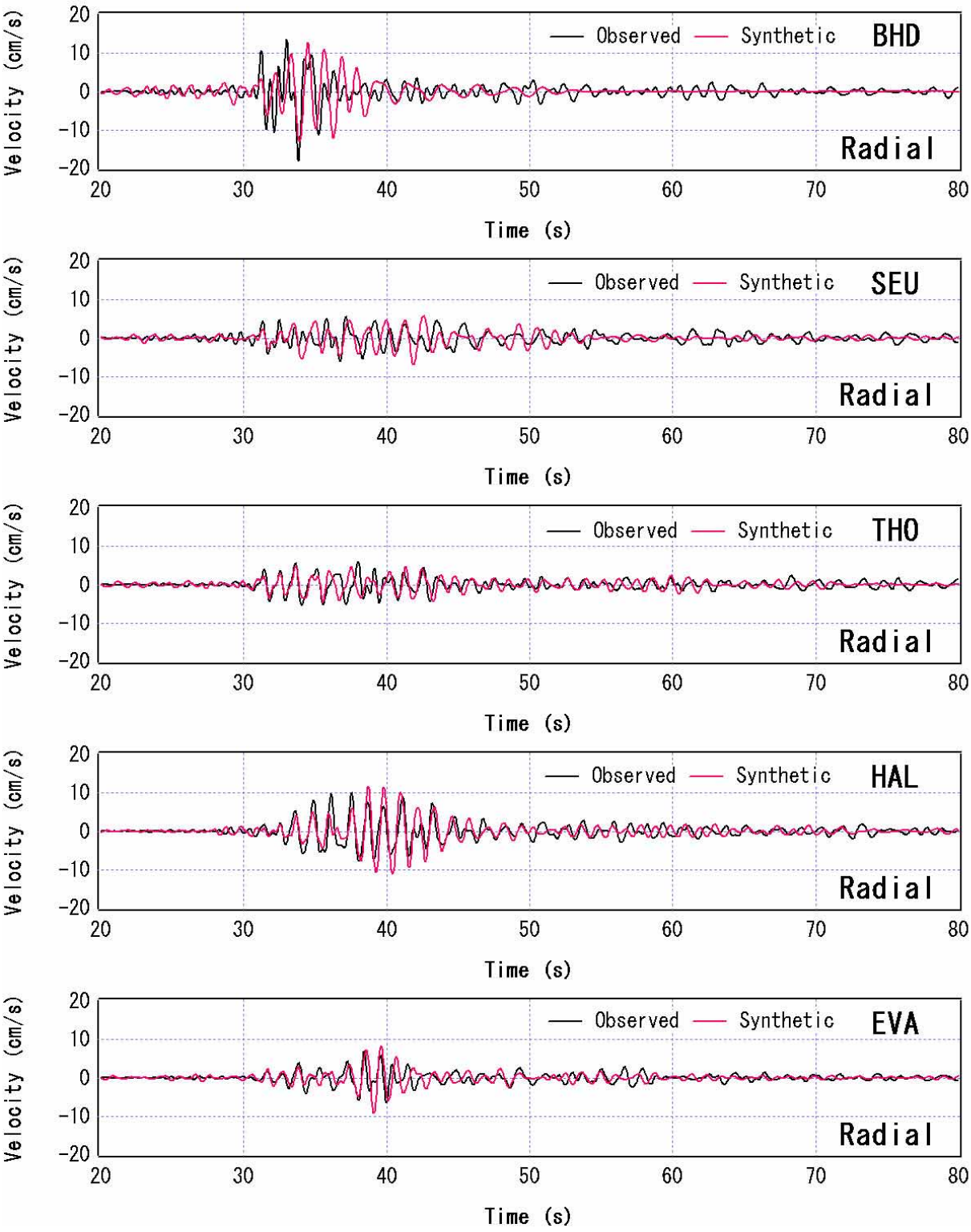

Figure 9 Observed and synthetic ground velocities at Pleistocene stiff-soil sites. In the simulation, nonlinear parameters listed in Table 2 are used.

Sites on Artificial fill

The same analysis was applied to sites on artificial fill, namely, HAR, SDN and SDS, to assess the effects of soil nonlinearity.

At first, the mainshock velocity at HAR was synthesized by using the source model without consideration of soil nonlinearity. The result is compared with the observed velocity in **Figure 10(a)**. It can be seen that the amplitude and the duration of excitation is apparently overestimated especially for the later phases. The discrepancy is much more serious than for the stiff-soil sites (**Figure 5** and **Figure 8**), indicating the importance of soil nonlinearity for this site. If it were not for soil nonlinearity, peak ground velocity at HAR could have been over 40 cm/s during the mainshock. Then, the ground velocity was synthesized with consideration of soil nonlinearity. The nonlinear parameters ν_1=0.66 and ν_2=0.02 at 1 Hz were used. The values correspond to the decrease in shear wave velocity by a factor of 0.66 and the increase in damping factor of 0.02 at 1 Hz. Synthetic velocity at HAR was much improved by incorporating "nonlinear parameters" as shown in **Figure 10(b)**. The duration and the peak amplitude approached to that of the observed velocity. The phases for the later arrivals (35-45 seconds in **Figure 10**) were also improved. Frankel [6] anticipated that the resonant frequency at 0.6 Hz for a weak motion at HAR shifted to 0.45 Hz during the mainshock. This corresponds to a decrease in shear wave velocity by a factor of 0.75, which is fairly consistent with the value ν_1 used for our simulation (0.66) if we consider the degree of smoothing adopted for spectral ratio analysis [6]. The authors have to admit that coincidence between the observed and the synthetic ground velocities is not perfect. Especially, there is still a discrepancy in the amplitude around 30-35 seconds. This is probably due to the nonstationarity of the material properties, which is neglected in our modeling. Frankel [6] pointed out several indications for nearby liquefaction at this station. It implies the nonstationarity of the material properties at the site, which cannot be sufficiently addressed with the method used.

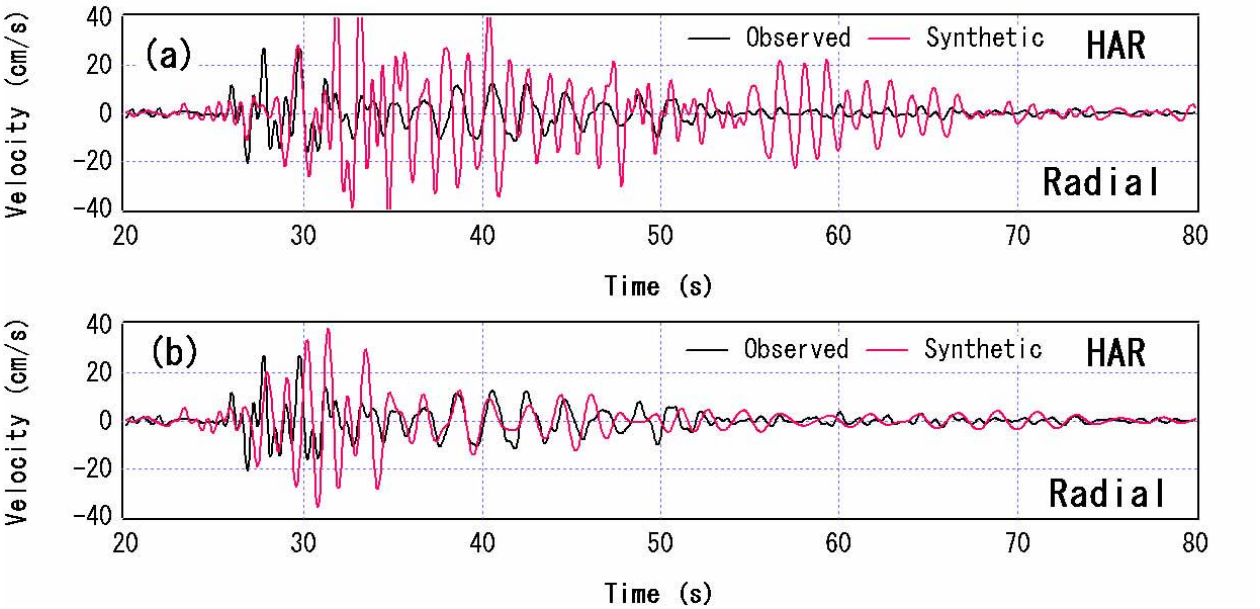

Figure 10 Observed and synthetic ground velocities at HAR on artificial fill. (a) Soil nonlinearity is neglected. (b) Nonlinear parameters listed in Table 2 are used.

Similar analyses were conducted for sites SDN and SDS, also located on artificial fill. These are the sites that constitutes SD array south of downtown [6]. Another SD array station SDW was excluded from the analysis because the Green's function was not available. Liquefaction was found about 100m from the station SDN [6]. The station SDS had nearby liquefaction [6]. The accelerogram at SDS was characterized by cusped arrivals [6], which is an indication of soil nonlinearity.

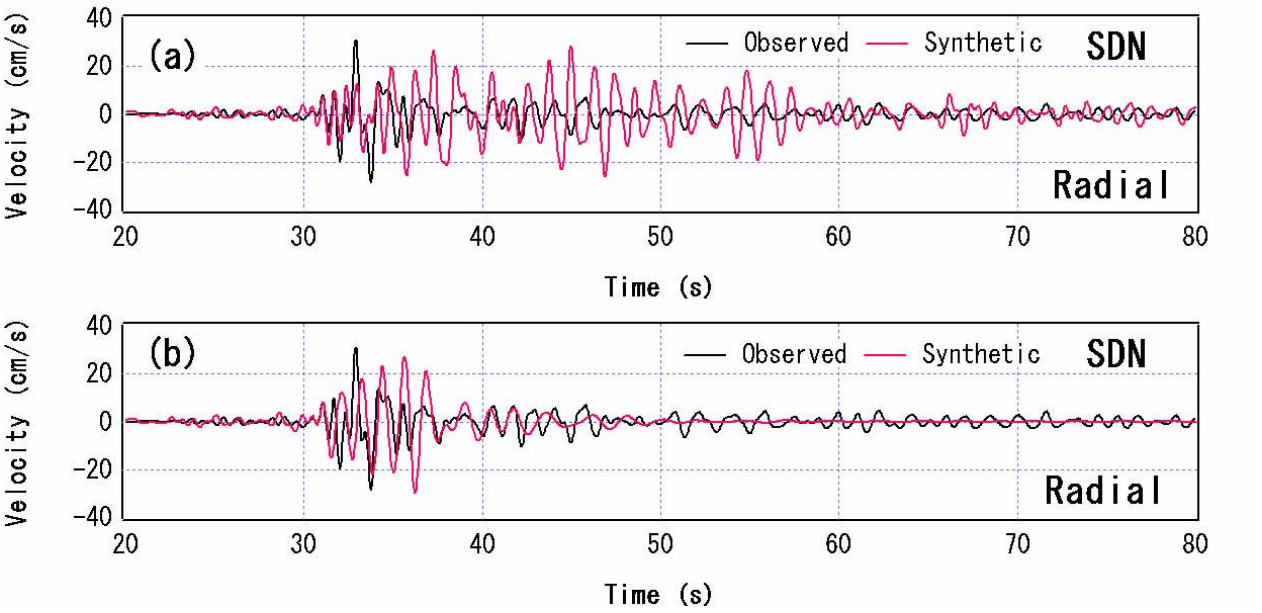

Figure 11 Observed and synthetic ground velocities at SDN on artificial fill. (a) Soil nonlinearity is neglected. (b) Nonlinear parameters listed in Table 2 are used.

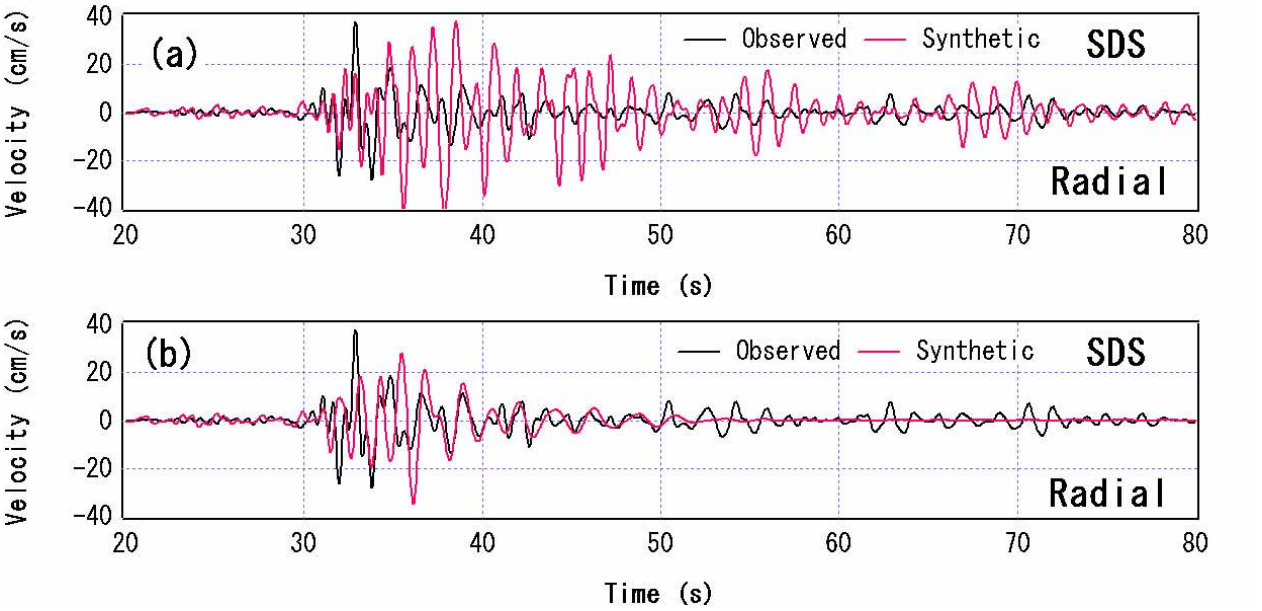

Figure 12 Observed and synthetic ground velocities at SDS on artificial fill. (a) Soil nonlinearity is neglected. (b) Nonlinear parameters listed in Table 2 are used.

Synthetic velocities that does not account for soil nonlinearity are characterised by a very long duration of excitation for more than 30 seconds (**Figure 11(a)** and **Figure 12(a)**), which is not the case for the observed velocities. Then, the ground velocity was synthesized with consideration of soil nonlinearity. The nonlinear parameters ν_1=0.65-0.68 and ν_2=0.06 at 1 Hz were used. The values correspond to the decrease in shear wave velocity by a factor of 0.65-0.68 and the increase in damping factor of 0.06 at 1 Hz. Synthetic velocities at both stations were much improved by incorporating "nonlinear parameters" as shown in **Figure 11(b)** and **Figure 12(b)**. The duration of excitation approached to that of the observed

velocities. Frankel [6] anticipated that the resonant frequency at 0.65 Hz for a weak motion at SDS shifted to 0.35 Hz during the mainshock. This corresponds to a decrease in shear wave velocity by a factor of 0.54, which is fairly consistent with the value ν_1 used for our simulation at SDS (0.65). The authors have to admit that coincidence between the observed and the synthetic ground velocities is not perfect. Especially, there is still a discrepancy in the amplitude around 35 seconds. This is again probably due to the nonstationarity of the material properties, which is neglected in our modeling.

CONCLUSIONS

In this study, the effects of soil nonlinearity in the Seattle Basin during the 2001 Nisqually, Washington, earthquake (M_W6.8) were assessed by using the empirical Green's function method.

First, a waveform inversion was conducted to construct a source model appropriate for use in the empirical Green's function method. In the inversion, some of the records on Pleistocene stiff soils were used. Only portions with durations of 5 seconds including the S waves were used for the inversion. Recordings from the M_L3.4 aftershock were used as the Green's functions. The source model thus obtained can explain the S waves not only at the sites used for the inversion but also at stiff-soil sites that were not included in the inversion.

Secondly, the source model was used to assess the effects of soil nonlinearity on the later phases of the records at Pleistocene stiff-soils sites. The amplitudes of the later phases tend to be overestimated even at stiff-soil sites if soil nonlinearity is neglected in the analysis. Then simulations were conducted to incorporate soil nonlinearity by introducing "nonlinear parameters" in the empirical Green's function method. It was found that the synthetic velocities approach to the observed ones by introducing nonlinear parameters. At some of these sites, although increase in the damping factor was small (0.005), its effects on the amplitude of the later phases were not negligible. This is presumably due to the fact that the rays corresponding to the later phases are trapped within the sedimentary basin for a long time.

Finally, the source model was used to assess the effects of soil nonlinearity on the records at soft-soil sites on artificial fill. The amplitudes of the later phases were dramatically overestimated at these sites if soil nonlinearity is neglected in the analysis. The discrepancies are much more serious than for the stiff-soil sites, indicating the importance of soil nonlinearity for these sites. Then simulations were conducted to incorporate soil nonlinearity by introducing "nonlinear parameters". Synthetic velocities at these sites were much improved by incorporating "nonlinear parameters". The durations and the peak amplitudes approached to those of the observed velocities.

The results emphasize the importance of the effects of soil nonlinearity on the later phases of strong ground motions, which have not been sufficiently addressed so far. Efforts are needed to establish a reasonable way to evaluate such effects to avoid overestimation of the later phases in the prediction of ground motion for future large earthquakes at sites in a sedimentary basin.

ACKNOWLEDGMENTS

The authors would like to express their sincere gratitude to the U.S. Geological Survey who generously provided the data from the Seattle Urban Seismic Array (http://groundmotion.cr.usgs.gov). The authors would like to thank Momoyo Kitamura for assistance in preparing manuscripts.

REFERENCES

1. Aki K. "Local site effects on weak and strong ground motion." Tectonophysics 1993; 218: 93-111.
2. Beresnev IA, Wen KL. "Nonlinear soil response: a reality?" Bull Seism Soc Am 1996; 86: 1964-1978.

3. Nozu A, Morikawa H. "An empirical Green's function method considering multiple nonlinear effects." Zisin 2003; 55: 361-374.
4. Hartzell SH. "Earthquake aftershock as Green's functions." Geophys Res Lett 1978; 5: 104.
5. Irikura K. "Prediction of strong acceleration motion using empirical Green's function." Proceedings of the 7th Japan Earthquake Engineering Symposium 1986: 151-156.
6. Frankel AD, Carver DL, Williams RA. "Nonlinear and linear site response and basin effects in Seattle for the M6.8 Nisqually, Washington, earthquake." Bull Seism Soc Am 2002; 92: 2090-2109.
7. Schnabel PB, Lysmer J, Seed HB. "SHAKE - A computer program for earthquake response analysis of horizontally layered sites." Report No. EERC 72-12, Col. of Eng., University of California at Berkeley 1972.
8. Hartzell SH, Heaton TH. "Inversion of strong ground motion and teleseismic waveform data for the fault rupture history of the 1979 Imperial Valley, California, Earthquake." Bull Seism Soc Am 1983; 73: 1553-1583.
9. Lowson CL, Hanson RJ. "Solving least squares problems." Englewood Cliffs: Prentice-Hall, Inc., 1974.